Int J Clin Exp Med 2018;11(7):6583-6595
www.ijcem.com /ISSN:1940-5901/IJCEM0077046

Original Article

Effects of MCPH1 silencing on proliferation, apoptosis, and chemo-sensitivity of non-small cell lung cancer cells

Li Wei[1], Qiang Zhang[2], Xinli Wang[3], Xia An[1], Qian Han[1], Ling Meng[1], Wenwen Cao[1]

Departments of [1]Respiratory Medicine, [2]Thoracic Surgery, [3]Pathology, Affiliated Hospital of Taishan Medical University, Taian City, Shandong Province, P. R. China

Received March 30, 2018; Accepted April 27, 2018; Epub July 15, 2018; Published July 30, 2018

Abstract: Objective: The aim of this study was to elucidate the effects of MCPH1 silencing on proliferation, apoptosis, and chemo-sensitivity of non-small cell lung cancer cells. Methods: Specimens were pooled from 50 cases of confirmed non-small cell lung cancers and 20 cases of normal lung tissues. Pathological changes in the tissues of the two groups were observed using HE staining. Positive rates of MCPH1 protein expression in lung cancer tissues and normal lung tissues were detected by immunohistochemistry. Loss status of MCPH1 at 3 loci in lung cancer tissues was determined by comparative genomic hybridization (CGH) assay and loss of heterozygosity (LOH) of MCPH1 in lung cancer tissues was also measured. The cultured cells were disassociated and stratified into normal lung cells (Normal), lung cancer cells (Blank), lung cancer cells as negative controls (NC), lung cancer cells with MCPH1 overexpression (MCPH1 mimic), and lung cancer cells with MCPH1 knockout (siRNA-MCPH1). Protein and mRNA expression of MCPH1, PARP1, POLD1, PRKDC, Bax and Bcl-2 were detected by qRT-PCR and Western blot. MTT assay and flow cytometry were applied to determine cell proliferation, apoptosis, and cycle distribution of each group, after transfection, and semi-inhibitory concentrations (IC_{50}) of cisplatin and paclitaxel in all groups of cells for evaluation of chemotherapy sensitivity. Results: Compared to normal lung tissue, MCPH1 protein positive expression was significantly reduced in non-small cell lung cancer tissues. CGH detection indicated multiple chromosomal aberrations in 50 specimens of lung cancer tissue. The mean number of chromosomal aberrations was 11.2. Analysis of LOH at the MPCH1 microsatellite loci showed that LOH was found in at least one locus in 39 specimens (78%), 24 specimens (61.53%) of which had LOH in all 3 loci. When compared with the Normal subset, protein and mRNA expression of MCPH1 and Bax and apoptosis rates of cells were decreased remarkably. Rates of cells in G1 phase were lowered considerably, but substantive increases were noted in protein and mRNA expression of PARP1, Bcl-2, POLD1 and PRKDC. There were increases in cell proliferation as well as IC_{50} values of cisplatin and paclitaxel in remaining cell subsets. When compared with Blank and NC subsets, MCPH1, Bax protein and mRNA expression, and apoptosis rates of cells and rates of cells in the G1 phase were elevated considerably, but protein and mRNA expression of PARP1, PRKDC, POLD1 and Bcl-2, proliferation rates of cells, and IC_{50} values of cisplatin and paclitaxel were reduced significantly in the MCPH1 mimic subset. Protein and mRNA expression of MCPH1 and Bax, apoptosis rates, and rates of cells in G1 phase in the siRNA-MCPH1 subset were reduced considerably, but protein and mRNA expression of PARP1, PRKDC, POLD1, Bcl-2, cell proliferation, and IC_{50} values of cisplatin and paclitaxel were increased in the siRNA-MCPH1 subset. Conclusion: Silencing of MCPH1 genes significantly accelerates proliferation of non-small cell lung cancer cells, reducing apoptosis and sensitivity of cells to chemotherapy.

Keywords: MCPH1, non-small cell lung cancer, proliferation, apoptosis, chemo-sensitivity

Introduction

Lung cancer is one of the most common malignancies causing the most deaths in the world [1-2]. Inadequate early diagnosis and treatment is a crucial cause for its high mortality and threat to human health [3]. Microcephalin (MCPH1) is a gene associated with human small heads. Mutation of MCPH1 is a major cause of primary microcephaly [4]. Current research has confirmed that MCPH1 is involved in an assortment of cell activities including DNA damage response, cell cycle regulation, and tumor growth. Low expression or absence of MCPH1 has been closely linked with onset and development of tumors [5-7].

Mantere et al. found that MCPH1 is closely related to apoptosis of breast cancer cells. Overexpression of MCPH1 may promote apop-

tosis of breast cancer cells and lay the basis for the mechanism of action of MCPH1 in apoptosis of breast cancer cells [8]. After transfection of human lung cancer A549 cells, Wenting et al. found that overexpression of MCPH1 inhibited the migration and invasion of lung cancer cells, suggesting that MCPH1 can be used as a new target for diagnosis and treatment of lung cancer [9]. With in depth research on molecular biology, growing evidence has shown that sequence of genes related to lung cancer or changes in base numbers affect the transcription of genes and biological behavior of cells, leading to carcinogenesis or migration of cells. Loss of heterozygosity (LOH) refers the change to a pair of heterozygous alleles from a homozygous state. LOH is generally associated with tumor suppressor genes. When alleles are significantly absent or abnormal, they cannot suppress the malignant state and cells are transformed into cancer cells, accordingly. Therefore, this study was conducted to detect LOH of MCPH1 genes in lung cancer tissue and normal lung tissues. The aim of this study was to discuss the relationship between LOH of MCPH1 and occurrence of lung cancer.

Chemotherapy with cisplatin and paclitaxel is a frequently-used chemotherapy regimen for cancers. Nevertheless, decreased sensitivity of tumor cells to chemotherapy adversely affects the efficacy of chemotherapy [10]. RNA interference technology was applied to clarify the effects of silencing of MCPH1 genes on sensitivity of cells to chemotherapy with cisplatin and paclitaxel in non-small cell lung cancers. This study aimed to bring insight into clinical work and lay a foundation for further investigating the impacts of silencing of MCPH1 genes on proliferation, apoptosis, and chemo-sensitivity of cells in non-small cell lung cancers.

Methods and materials

Study patients

This experiment was done under the premise of safeguarding the interests of all participants. All participants were fully informed and, after ethical review, agreed to donate their medical records to the laboratories for research purposes. Between August 2015 and August 2016, 50 specimens of primary lung cancer tissue, pooled from patients with primary lung cancer from the Affiliated Hospital of Taishan Medical University, were assigned to the experiment group. Twenty specimens of normal lung tissue were assigned to the control group. No patients had undergone radiotherapy or chemotherapy before surgery. Among them, 21 patients had squamous cell carcinoma and 29 had lung adenocarcinoma. Patients were included if their pathological type was non-small cell lung cancer and if they had received no target treatment (such as radiotherapy and chemotherapy) before specimen collection. Specimens were placed into sterile EP-tubes without RNase immediately after being isolated from the patients. They were then placed into liquid nitrogen tanks and stored in a refrigerator at -80°C.

H&E staining

Specimens were fixed with 10% neutral formaldehyde solution for more than 24 hours. Subsequently, non-small cell lung cancer tissues and normal lung tissues were dehydrated with routine gradient alcohol (ethanol concentrations at 70%, 80%, 90%, 95% and 100%, respectively) at 1 min/time, transparentized with xylene twice (5 min each time), soaked and embedded in paraffin, and cut into 4 μm sections (some tissue sections were stored for following immunohistochemistry). The sliced tissue sections were baked in an oven at 80°C for 1 hours and then stained with hematoxylin (H8070-5 g, Beijing Solarbio Science Technology, China) for 4 minutes. After washing, the sections were differentiated with hydrochloric acid alcohol for 10 seconds, washed for 6 minutes, followed by bluing with aqueous ammonia for 8 minutes. Subsequently, they were stained with eosin solution (PT001, Shanghai Bogoo Biotechnology, China) for 3 minutes. After mounting with neutral balsam, sections were observed for cell histopathological changes (DMM-300D, Shanghai Caikon Optical Instrument, Shanghai, China) using an optical microscope.

Immunochemistry

Paraffin sections were baked in an oven overnight at 60°C, dewaxed with xylene, dehydrated in routine gradient alcohol (ethanol concentrations at 100%, 95%, 80% and 70%, respectively) for 5 minutes each, rinsed in tap water for 5 minutes, and washed 3 times with PBS for 3 minutes. Antigen retrieval was per-

Table 1. Primer sequences for microsatellite loci

Microsatellite loci	Sequence
D3S1228	Forward: 5'-TCCTTAACTCTTTCTCTGTGAGTTG-3'
	Reverse: 5'-TCTACGAAAGGGATTAGGAAGGA-3'
D3S1029	Forward: 5'-TACCTCCTCACTGTTTCATATTAG-3'
	Reverse: 5'-CACATACTATGTCTCGGCTAACAG-3'
D9S171	Forward: 5'-AGCTAAGTGAACCTCATCTCTGTCT-3'
	Reverse: 5'-ACCCTAGCACTGATGGTATAGTCT-3'

formed in 0.01 M citrate buffer for 10 minutes and then sections were placed in 0.3% H_2O_2-methanol solution for 20 minutes. MCPH1 antibodies (1:300, ab2612, Abcam, Inc, MA, USA) were added and PBS served as negative control. HRP-conjugated goat anti-rabbit IgG (1:1000, ab6721, Abcam) was used as secondary antibody. Sections were visualized with a DAB substrate for 5 minutes (P0203, Beyotime Biotechnology, Shanghai, China) and the degree of visualization was controlled using a microscope. Sections were mounted with neutral resin and observed and photographed using a microscope. Five fields were chosen for each section. Cells were positive when the cytoplasm or nucleoplasm was brownish. Positively stained cells in each field were counted by randomly selecting 5 fields for each section. Positively stained cells in each field and the positive rates of cells were calculated using Image-Pro Plus, version 7.0.

Comparative genomic hybridization

Comparative genomic hybridization (CGH), also known as DNA copy number karyotype technique, was used to detect relative DNA copy number changes between genomes. The method was as follows: DNA was extracted from lung cancer tissues using kits and dissolved in TE solution. After that, 1 μg of genomic DNA, 10 μL of dNTP mix, 5 μL of 0.1 mmol/LdTTP, 6 μL of 10x nick translation enzyme buffer, 8 μL of nick translation enzyme, and 2.5 μL of Spectrum Green dUTP at 0.2 mmol/L were added to the centrifuge tubes. Deionized water was added to each test tube so that the total volume of solution in each test tube was 50 μL. The solution was incubated in water at 18°C for 2 hours and then an additional water bath at 65°C for 10 minutes. Subsequently, the reaction was terminated and the tubes were placed on ice for storage. Mixed probes were prepared, centrifuged, the supernatant discarded, and 7 μL of purified water was added to the CGH hybridization buffer. *In situ* hybridization was performed as follows: probes were denaturized in formamide at 72°C for 2 minutes, soaked in alcohol at the respective purity of 70%, 85% and 100% for 1 minute each, and air-dried. Afterward, 10 μL of mixed probes was added dropwise and hybridized for 72 hours at 37°C; 10 μL of LDAPIII counterstain was added for counterstaining. Two hours later, the slides were observed under a microscope. The probe primer sequence was F: 5'-AGTGGGAGACGCAAAAAGCC-3', R: 5'-GTTCGAACGGCTCCTCAGAA-3'. Image acquisition was performed using an AI image acquisition system. Images were acquired at no less than 20 acquired sites. Chromosome deletions and amplifications were determined using the ratio of two fluorescence hybridization signals displayed on the cytovision system.

Loss of heterozygosity detection

Cancer tissues and cancer-adjacent normal tissues (100 mg for each) were taken, grounded, and digested with proteinase K, followed by DNA extraction. After DNA extraction, extracted DNA was determined for content and concentration by an ultraviolet spectrophotometer, then diluted to 0.1 μg/Ml and stored at -40°C. Three microsatellite loci (including D9S171, D3S1228, and D3S1029) near MCPH1 were selected, according to Genome Date Base (GDB) https://www.ncbi.nlm.nih.gov/genome/. The corresponding forward and reverse strand primers were designed with the use of online primer design software (Primer 3) (**Table 1**). PCR was performed in a total reaction volume of 20 μL and the PCR program was Touchdown. PCR was conducted under the following cycling conditions: initial 11 cycles of thermal cycling at 92°C for 15 minutes, denaturation at 91°C for 20 seconds, annealing at 64°C for 40 seconds, extension at 67°C for 2 minutes; followed by 24 cycles of denaturation at 92°C for 20 seconds, annealing at 54°C for 40 seconds, extension at 68°C for 2 minutes, and 62°C for 1 hour. LOH analysis was made as follows: products from genomic DNA amplification, which had been collected from the tissues, were diluted 20-fold and 10 μL of LIZ500 diluent was added to the PCR multi-well plates. The diluted PCR products were mixed evenly by agi-

Table 2. qRT-PC primer sequences

Gene	Sequence
MCPH1	Forward: 5'-CACCATCTTTCACTCACCTC-3'
	Reverse: 5'-CTTACTGAGGAACTCCTGG-3'
PARP1	Forward: 5'-AAGAAGCCAACATCTGAGCT-3'
	Reverse: 5'-TTTCCTTGTCATCCTTCAGC-3'
POLD1	Forward: 5'-CTCCTTAGGTCCTGGTCTACATG-3'
	Reverse: 5'-GCTCCGCTCCTACACGATCAA-3'
PRKDC	Forward: 5'-ACTCCAAGATGCTCCTACCTC-3'
	Forward: 5'-ACATGTAGCTGCTTTCTTACGG-3'
Bax	Forward: 5'-GGCCCACCAGCTCTGAGCAGA-3'
	Forward: 5'-GCCACGTGGGCGTCCCAAAGT-3'
Bcl-2	Forward: 5'-GTGGAGGAGCTCTTCAGGGA-3'
	Forward: 5'-AGGCACCCAGGGTGATGCAA-3'
GAPDH	Forward: 5'-GGTGTGAACCACGAGAAATATGAC-3'
	Forward: 5'-TCATGAGCCCTTCCACAATG-3'

tation. Electrophoresis was performed using an ABI3130xl sequencer. Data in the experiment were analyzed using GeneMapper 4.0. LOH was identified when tumor tissues showed more than 33% absence of PCR product bands of DNA compared to cancer-adjacent tissues.

Cell culture

Approximately 3 mm of lung tissue was extracted from each patient with lung adenocarcinoma in the experiment group. The tissue was rinsed with D-Hanks and the supernatant was removed. After addition of DMEM medium containing 0.15% collagenase, the lung tissue was transferred to a sterile test tube, digested in an incubator for 30 minutes at 37°C, and centrifuged at 700 r/min for 6 minutes. The supernatant was removed. After addition of DMEM low-glucose medium containing 20% fetal bovine serum (FBS), tissue was centrifuged for 6 minutes at 700 r/min. Cell suspension was prepared by placing sediments into a culture medium. Subsequently, cell suspension was transferred to a Petri dish and digested for 9 minutes in an incubator at 37°C in 5% CO_2, after addition of an appropriate amount of 0.2% trypsin containing 0.01% EDTA. Digestion was terminated by adding culture medium containing 25% FBS. The suspension was centrifuged for 5 minutes at 1200 r/min and then the supernatant was pipetted. Cells were resuspended in DMEM medium containing 25% FBS, transferred to a new Petri dish, and cultured in an incubator at 37°C in 5% CO_2, with the culture medium replaced every 2 days.

Normal lung tissues (approximately 3 mm) were extracted from controls, washed once with 0.25% trypsin solution, and digested with 0.25% trypsin for 10-20 minutes. After addition of DMEM medium containing 10% FBS, cryogenic centrifugation was performed at 1,500 r/min for 5 minutes and then supernatant was removed. The sediments were added to 0.1% type I collagenase, digested for 10-20 minutes, and centrifuged at 1,000 r/min for 5 minutes after addition of DMEM medium containing 10% FBS. Cell suspension was seeded into a culture flask, cultured in an incubator at 37°C in 5% CO_2 for 40 minutes, centrifuged at 800 r/min for 5 minutes, and then the supernatant was removed. After addition of DMEM medium containing 10% FBS, the precipitated cells, namely lung epithelial cells, were resuspended, seeded in a culture flask, and cultured in an incubator at 37°C in an atmosphere of 5% CO_2.

Cell stratification and transfection

Third-generation cells were stratified into 5 subsets: Normal subset (normal lung epithelial cells without transfection with any sequence), Blank subset (lung adenocarcinoma cells without transfection with any sequence), negative control (NC) subset (lung adenocarcinoma cells, transfected with negative control), MCPH1 mimic subset (lung adenocarcinoma cells transfected with MCPH1 mimic), and siRNA-MCPH1 subset (lung adenocarcinoma cells transfected with siRNA-MCPH1). Cells in logarithmic phase in the Normal, Blank, negative control (NC), MCPH1 mimic, and siRNA-MCPH1 subsets were seeded in 6-well plates. Once the cells reached 40-50% confluence, they were transfected, according to instructions for Lipofectamine 2000 (Invitrogen, Carlsbad, CA, USA). Subsequently, 100 pmol of MCPH1 mimic, siRNA-MCPH1, and negative control (final concentration 50 nM when added in cells) were diluted with 250 μL of serum-free medium Opti-MEM (Gibco, Grand Island, NY, USA) and mixed and incubated at room temperature for 5 minutes. Then, 5 μL of Lipofectamine 2000 was diluted with 250 μL of serum-free medium Opti-MEM, mixed and incubated at room temperature for 5 minutes. The above two generated compounds were mixed and incubated for

20 minutes, transferred to culture wells, and cultured at 37°C in 5% CO_2. The medium was thoroughly replaced 6-8 hours later. Cells were cultured for additional 48 hours for subsequent experiments.

qRT-PCR

Total RNA was extracted following instructions for the RNA extraction kits (D203-01, GenStar BioSolutions, Beijing, China). Reverse transcription to cDNA was performed following the instructions of TaqMan MicroRNA Assays Reverse Transcription Primers (4427975, Applied Biosystems, USA). Reverse transcribed cDNA was diluted to 50 mg/μL with 2 μL added each time. Reaction amplification system was 25 μL. The conditions for reverse transcription reaction were as follows: 37°C for 20 minutes; 83°C for 10 seconds. Primers miRNA-374b, JAM-2, and ERK were synthesized by TaKaRa (**Table 2**). Real-time quantitative PCR was carried out on a 7500 ABI Prism Sequence Detection System (7500, ABI, USA) under the following cycling conditions: pre-denaturation at 95°C for 9 minutes, denaturation at 95°C for 20 seconds, annealing at 62°C for 15 seconds, extension at 72°C for 35 seconds, for a total of 45 cycles. qPCR was determined in a 20 μL reaction mixture containing SYBR® Premix Ex Taq™ II (2x) 10 μL, 0.8 μL of PCR Forward Primer (10 μL), 0.8 μL of Uni-miR qPCR Primer (10 μL), and ROX Reference Dye (50x) 0.4 μL. The reverse transcription yielded 2 μL of cDNA template and 6 μL of ddH_2O. Expression levels of the target genes MCPH1, PARP1, POLD1, PRKDC, Bax, and Bcl-2 were calculated by $2^{-\Delta\Delta}$Ct method. Each essay was conducted in triplicate.

Western blot

Liquid nitrogen was added to extracted tissues. The tissues were ground into uniformly fine powder, followed by addition of 1 mL of tissue lysate (components: 60 mmol/L Tris, 140 mmol/L NaCl, 5 mmol/L EDTTA, 0.1% SDS, 2% NP-40, 5 μg/mL Aprotinin, and 1 mmol/L PMSF). The mixture was incubated on ice and homogenized, with protein lysate added at 4°C, lysed for 30 minutes, and agitated once every 15 minutes. This was followed by centrifugation at 4°C for 30 minutes at 12,000 r/min. After the lipid layer was removed, the supernatant was taken. Protein concentration was measured using BCA kits (20201ES76, Yeasen Biotech, Shanghai, China) and 25 μg of protein lanes were adjusted with deionized water. Concentrated gels and 10% SDS isolated gels were prepared. The samples were mixed with sampled buffer and boiled for 5 minutes at 100°C. After culturing on ice and centrifugation, equal amounts of protein were added with a micropipette to each lane for electrophoretic separation and then proteins on the gels were transferred onto PVDF membranes. Subsequently, the membranes were blocked with 4% skimmed milk powder at 4°C for 2 hours. They were incubated with rabbit anti-human MCPH1 (1:500, ab2612, Abcam, Cambridge Science Park, UK), POLD1 (1:1000, ab186407, Abcam, Cambridge Science Park, UK), PARP1 (1:1000, ab32064, Abcam, Cambridge Science Park, UK), PRKDC (1:1000, Ab32566, Abcam, Cambridge Science Park, UK), BAX (1:250, Ab325-03, Abcam, Cambridge Science Park, UK), BCL-2 (1:1000, Ab32124, Abcam, Cambridge Science Park, UK), and HRP-conjugated rabbit anti-human GAPDH antibodies (internal reference) (ab9485, Abcam, Cambridge Science Park, UK) overnight at 4°C, Membranes were washed 3 times for 3 minutes and incubated with HRP-conjugated goat anti-rabbit secondary antibodies (diluted at 1:5000, P0265, Beyotime Biotechnology, Shanghai, China). Proteins were visualized using enhanced chemiluminescence (ECL) detection system. The expression content of each protein was semi-quantitatively represented by the ratio of A (absorbance) value of the protein to A value of GAPDH.

Cell proliferation after transfection tested by MTT assay

Once the cells of each subset reached approximately 80% confluence, they were rinsed twice with PBS and digested with 0.5% trypsin to prepare single-cell suspension. Cells were plated in 96-well plates at a density of $4 * 10^3$ to $6 * 10^3$ cells per well. Each well had a volume of 0.2 mL. The plates were incubated in a constant temperature incubator at 37°C. After 48 hours of incubation, the plates were taken out and cultured in culture medium containing 10% MTT solution (5 g/L; GD-Y1317, Shguduo, Shanghai, China) for an additional 4 hours. The supernatant was discarded and 100 μL of DMSO (D5879-100ML, Sigma, USA) was added

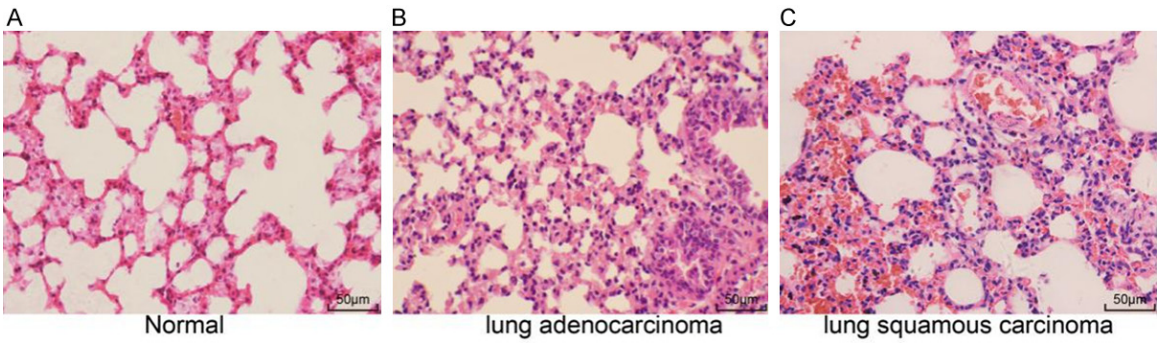

Figure 1. HE staining for non-small cell lung cancer and normal lung tissues (200×). A: Normal cancer-adjacent tissue; B: Lung adenocarcinoma tissue; C: Lung phosphorous carcinoma tissue.

to each well, followed by 10 minutes of agitation. Subsequently, absorbance of each well at 490 nm was measured with use of a microplate reader (Nanjing DeTie Laboratory Equipment, Nanjing, China). Each test was performed in triplicate. Cell viability curves were plotted with time points as the x axis and OD values as the y axis.

Cell apoptosis and cycles detected by flow cytometry

The apoptosis profile of the cells was determined by annexin V-FITC/PI double staining. After 48 hours of culturing, the cells were digested with 0.25% trypsin solution, incubat ed for 48 hours at 37°C in an atmosphere of 5% CO_2, washed twice with PBS, centrifuged, and resuspended in 200 μL of binding buffer. After addition of 15 μL of annexin V-FITC and 10 μL of PI, they were mixed, and reacted at room temperature for 10 minutes; 300 μL of binding buffer was added and then the apoptosis profile of the cells was measured using a flow cytometer (6HT, Cellwar Bio-technology, Wuhan, China).

After 48 hours of transfection, medium was removed and cells were washed once with PBS, digested in 0.25% trypsin, harvested, and centrifuged at 4°C for 5 minutes at 1000 r/min. The supernatant was discarded. Cells were rinsed twice with pre-cooled balanced salt solution PBS, centrifuged for 5 minutes at 1000 r/min, and the supernatant was removed. Prechilled 70% ethanol was added to fix the cells overnight at 4°C. After cells were rinsed with balanced salt solution PBS, they were centrifuged for 5 minutes at 1,000 r/min. Subsequently, 10 μL of RNase enzyme was added to incubate the cells at 37°C for 5 minutes and 1% PI (40710ES03, Shanghai Qcbio Science & Technologies, China) was added to stain the cells away from light for 30 minutes. Samples were placed on a flow cytometer (FACSCalibur, BD, FL, NJ, USA). Red-fluorescent signals at the excitation wavelength of 488 nm were recorded for detection of cell cycles. Each experiment was performed in triplicate.

Cell sensitivity to chemotherapeutic drugs

Cells in logarithmic phase of all subsets were seeded in 96-well plates at 3 * 10^3 to 6 * 10^3 per well, with 6 paralleled wells in each subset. After adherence to the surface of each well, cisplatin at seven concentrations of 0.03, 0.3, 0.75, 1.5, 3, 10 and 30 μg/mL and paclitaxel at 0.000, 5, 0.005, 0.05, 0.5, 5, 10 and 25 μg/mL were added to each well. Plates were incubated for 6 hours at 37°C in an atmosphere of 5% CO_2. Subsequently, the medium was replaced and plates were placed back into a consent temperature incubator and cultured for additional 48 hours; 25 μL of MTT (5 mg/mL) was added to each well and the plates were incubated for 3 hours in an incubator at 37°C in 5% CO_2. The medium was discarded, 150 μL of dimethyl sulfoxide was added to each well, then the plates were agitated for 10 minutes. Absorbance (A) values at 580 nm were measured on a Bio-Rad fluorescence microplate reader. The formula for calculating cell viability was as follows: Cell viability (%) = (A value of the experiment group/A value of the control group) * 10,000. Curve fitting was performed by SPSS (version 11.5) to calculate the half-inhibition concentration (IC_{50}) of cells at different concentrations of drugs.

Statistical analysis

Statistical data were processed with use of SPSS statistical software, version 22.0 (SPSS,

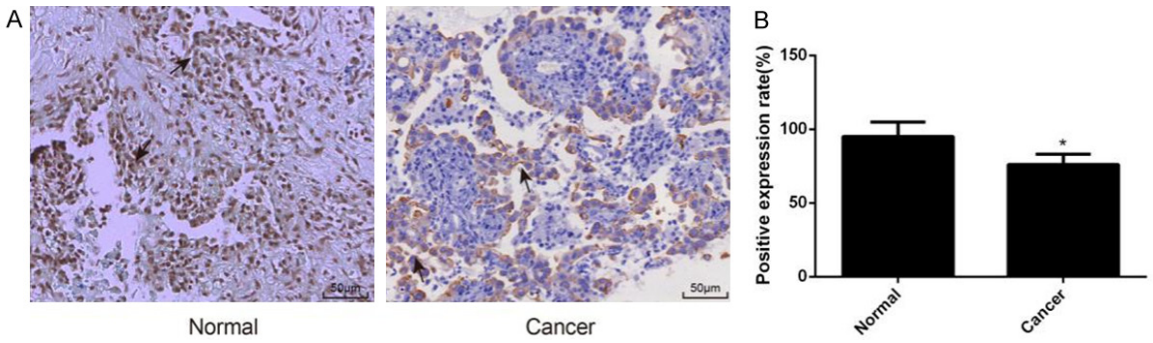

Figure 2. Immunohistochemical staining (200×). A: Normal lung tissue; B: Non-small cell lung cancer tissue MCPH1 protein positive expression rate in two cell subsets of tissue; *P<0.05, compared with normal subset.

Table 3. Deletion frequency in common deletion regions

Common deletion region	Chromosome deletion frequency
5q	26% (13/50)
6q	28% (14/50)
8q	50% (25/50)
9q	46% (23/50)

Inc, Chicago, IL, USA). Quantitative data are described as mean ± sd; t-tests were utilized for comparisons between two samples and one-way ANOVA with Bonferroni's post-hoc tests were applied for comparisons among more than two groups. Categorical data were measured by Pearson's correlation coefficient. Statistical significance was set as P<0.05.

Results

Pathological changes in non-small cell lung cancer tissues and tumor-adjacent normal lung tissues

HE staining indicated more type I alveolar cells in normal lung tissue and they were flat, smooth, no hairs, with oblate nuclei located in the core of cytoplasm. Type II alveolar cells were fewer. They were round or cubic. Small groups of type II alveolar cells were seen at the junctions of alveoli, with nuclei protruding to the cell surface (**Figure 1A**). Lung adenocarcinoma cells were heterogeneous, invasive or atypical, or heterogeneously infiltrated. Keratinization of single cells was observed, some arranged in real lumps or small cords, some with visible glandular cavities, and others arranged in tubular or adenoid structures. Intercellular bridges were seen between cancer cells and the nuclei were heterotypic, polymorphous, deep nuclear staining, and serrated at the borderline (**Figure 1B**). Additionally, columnar epithelial cells in lung squamous tissue had chronic irritation and damage, loss of cilia, squamous metaplasia of basal cells, hypoplasia, and dysplasia (**Figure 1C**).

MCPH1 protein expression of non-small cell lung cancer tissues and tumor-adjacent normal lung tissues

MCPH1 expression was identified in 38 of the 50 specimens of lung cancer tissue and in 19 of the 20 specimens of normal lung tissue. Immunohistochemical analysis demonstrated that MCPH1 proteins were strongly positive in normal lung tissues, in which MCPH1 was mainly expressed in the nuclei, whereas MCPH1 positive expression in lung ca ncer cells was positioned in the cytoplasm (**Figure 2A**, **2B**). The rate of MCPH1 positive expression was 95.00% in normal lung tissues and 76.00% in non-small cell lung cancer tissues. Hence, the rate of MCPH1 positive expression in lung cancer tissues was significantly lowered (t = 8.997, P<0.0001).

Chromosome deletion tested by CGH

Genomic DNA sequences of 50 specimens of non-small cell lung cancer (they were pathologically non-small cell lung cancers) were successfully analyzed using CGH. Almost every case was implicated in aberrations of multiple chromosomes. Among them, at least four chromosome aberrations were implicated. The most was 18 chromosome aberrations, with a mean of 11.2 chromosome aberrations per

Table 4. Loss of MCPH1 at microsatellite loci

	Microsatellite loci	LOH^+	LOH^-
Normal lung cancer	D3S1228	9	41
	D3S1029	11	39
	D9S171	7	43
	Frequency of at-least-one-locus LOH	22% (11/50)	
Lung cancer tissue	D3S1228	32	18
	D3S1029	37	13
	D9S171	34	16
	Frequency of at-least-one-locus LOH	78% (39/50)	

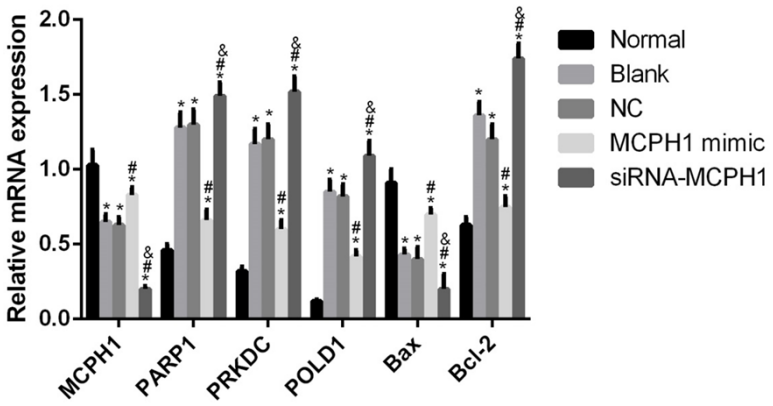

Figure 3. Comparison of mRNA expression of associated genes after transfection in various cell subsets. Note: *P<0.05, compared to the Normal subset; #P<0.05, compared with the Blank and NC subsets; &P<0.05, compared to the MCPH1 mimic subset.

specimen. Common amplification regions were 1, 11p, 16, and 19; common high-copy amplification regions were 1p11-1p13, 6p12-6p21, 16p11-16p12, 19p13 and 19q13; common deletion regions were 5q, 6q, 8q and 9q and frequencies are shown in **Table 3**.

LOH detection

Loss of MCPH1 at three loci in non-small cell lung cancer tissues and normal lung tissues is listed in **Table 4**. Among all 50 specimens of cancer tissue, 39 (78%) had LOH at least one locus, of which 24 (61.53%) had LOH at all 3 loci and the remaining 15 had LOH at one or two loci. Eleven specimens (22%) of normal tissue had LOH in at least one locus. LOH rate of MCPH1 at three loci (D3S1228, D3S1029 and D9S171) in specimens of lung cancer tissue was remarkably higher than in specimens of normal lung tissue (X^2 = 21.87, P<0.0001; X^2 = 27.08, P<0.0001; X^2 = 30.14, P<0.0001).

mRNA expression of relevant genes in cells after transfection

Results of qRT-PCR assay are displayed in **Figure 3**: Compared to Normal subset, mRNA expression levels of MCPH1 and Bax were reduced remarkably, but those of PARP1, PRKDC, POLD1, and Bcl-2 were elevated substantially in the remaining subsets (all P<0.05). When compared to the Blank subset, no great difference was noted in the changes of each gene in the NC subset. When compared to Blank and NC subsets, mRNA expression of MCPH1 and Bax in the MCPH1 mimic subset were elevated greatly, but those of PARP1, PRKDC, POLD1, and Bcl-2 were lowered strikingly (all P<0.05). mRNA expression levels of MCPH1 and Bax in the siRNA-MCPH1 subset dropped profoundly, but those of PARP1, PRKDC, POLD1 and Bcl-2 rose remarkably (all P<0.05). Compared to the MCPH1 mimic subset, mRNA expression levels of MCPH1 and Bax in the siRNA-MCPH1 subset decreased strikingly, but those of PARP1, PRKDC, POLD1 and Bcl-2 increased significantly (all P<0.05).

Protein expression of relevant genes in cells after transfection

Figure 4 shows the results of Western blot. Compared with the Normal subset, protein expression levels of MCPH1 and Bax in the remaining subsets were reduced remarkably, but those of PARP1, PRKDC, POLD1, and Bcl-2 were elevated significantly (all P<0.05). Compared to the Blank subset, no remarkable differences were noted in the changes of each gene in the NC subset. When compared to Blank and NC subsets, protein expression levels of MCPH1 and Bax were elevated strikingly, but those of PARP1, PRKDC, POLD1 and Bcl-2 were lowered remarkably in the MCPH1 mimic subset (all P<0.05); those of MCPH1

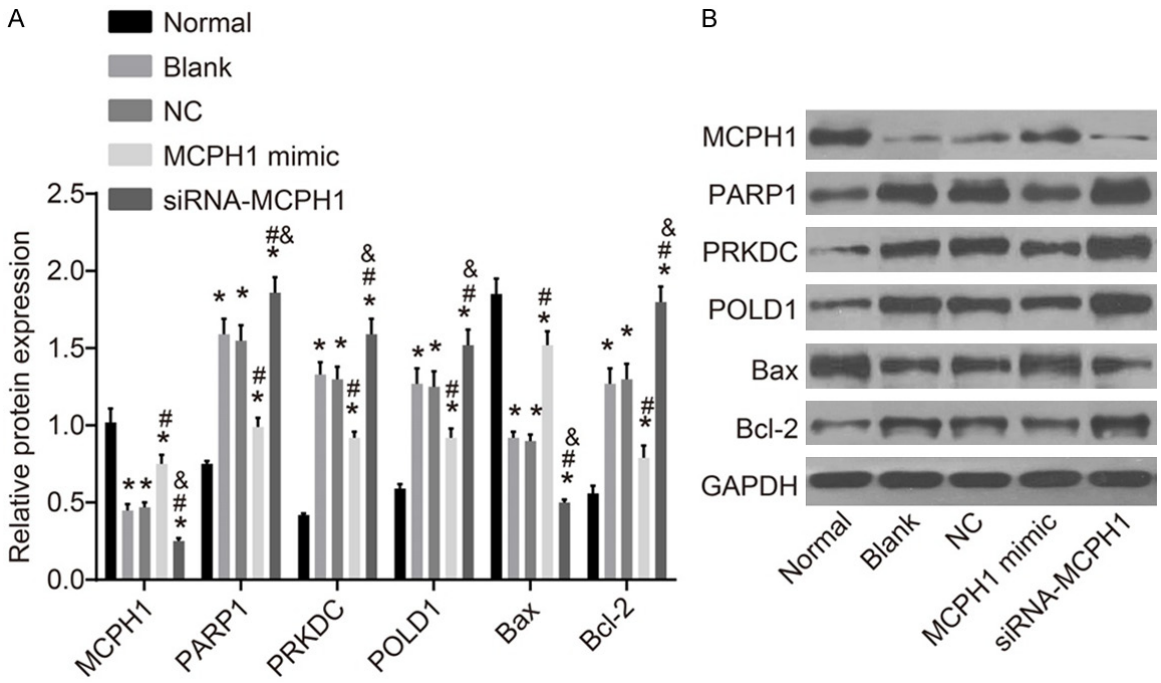

Figure 4. Protein expression levels of relevant genes after transfection in various cell subsets. Note: A: Protein expression of relevant genes in each cell subset; B: Graph of protein bands from western blot analysis; *P<0.05, compared to the Normal subset; #P<0.05, compared with the Blank and NC subsets; &P<0.05, compared to the MCPH1 mimic subset.

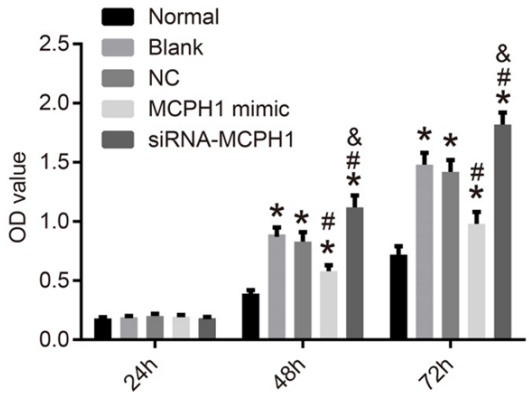

Figure 5. Cell proliferation in all subsets. Note: *P<0.05, compared with the Normal subset; #P<0.05, compared to the Blank and NC subsets; &P<0.05, compared with the MCPH1 mimic subset.

and Bax dropped substantially, but those of PARP1, PRKDC, POLD1, and Bcl-2 rose considerably in the siRNA-MCPH1 subset (all P<0.05). Compared to MCPH1 mimic subset, protein expression levels of MCPH1 and Bax were reduced remarkably, but those of PARP1, PRKDC, POLD1, Bcl-2 were elevated substantially in the siRNA-MCPH1 subset (all P<0.05).

Cell growth profile in all subsets

MTT assay (**Figure 5**) indicated no substantive differences in cell proliferation among the subsets after 24-hours of culturing. Nevertheless, proliferation of cells in the remaining cell subsets was remarkably higher than the Normal subset at 48 hours and 72 hours, respectively (both P<0.05). Proliferation of cells differed insignificantly between the Blank subset and the Normal subset, but proliferation of cells in the MCPH1 mimic subset dropped considerably compared to the Blank and NC subsets (P<0.05). Additionally, a significant increase in proliferation of cells was seen in the siRNA-MCPH1 subset (P<0.05).

Cell apoptosis detection

Figure 6 illustrates the findings of annexin V-FITC/PI double staining. Compared to the Normal subset, apoptosis rates of cells were lowered considerably in the remaining groups (all P<0.05). The Blank subset and NC subset varied insignificantly in apoptosis rates of cells. Apoptosis rates of cells rose remarkably in the MCPH1 mimic subset versus the Blank and the

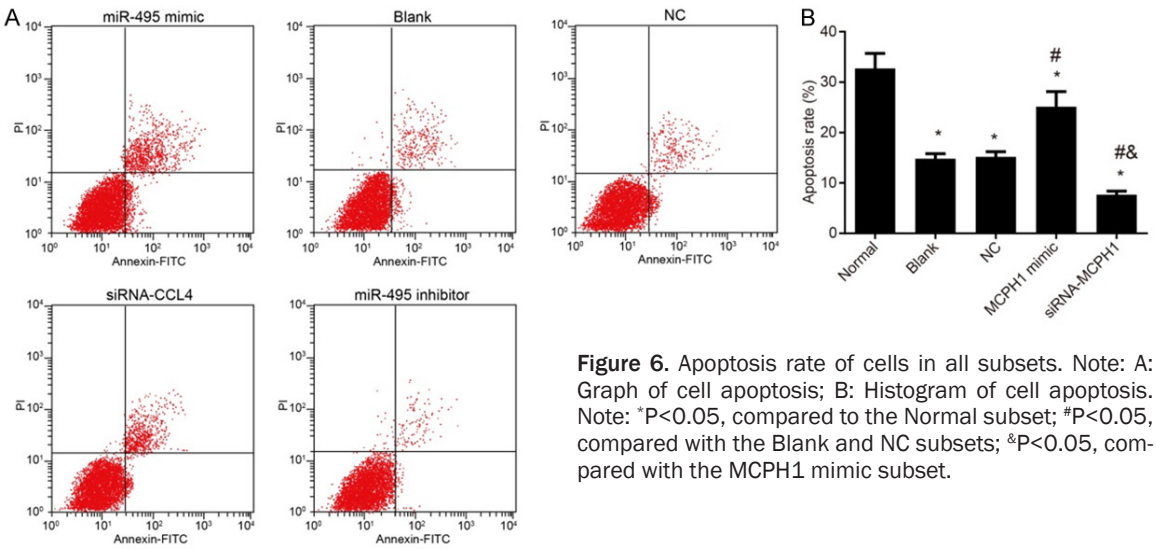

Figure 6. Apoptosis rate of cells in all subsets. Note: A: Graph of cell apoptosis; B: Histogram of cell apoptosis. Note: *P<0.05, compared to the Normal subset; #P<0.05, compared with the Blank and NC subsets; &P<0.05, compared with the MCPH1 mimic subset.

Table 5. IC_{50} of cells in all subsets

Subsets	Cisplatin (μg/mL)	Paclitaxel (μg/mL)
Normal	0.99±0.26	0.51±0.18
Blank	2.72±0.17*	1.17±0.19*
NC	2.74±0.12*	1.23±0.15*
MCPH1 mimic	1.91±0.15*,#	0.78±0.17*,#
siRNA-MCPH1	3.72±0.19*,#	1.62±0.22*,#

Note: *P<0.05, compared to the Normal subset; #P<0.05, compared with the Blank and NC subsets.

NC subsets (both P<0.05), but dropped substantially in the siRNA-MCPH1 subset (P<0.05).

Cell cycle distribution

According to results of cell cycle distribution testing (**Figure 7**), compared to the Normal subset, rates of cells in the G1 phase were reduced remarkably but those of cells in the S phase rose significantly in the remaining subsets (all P<0.05). No considerable differences between the NC subset and the Blank subset were seen in cell cycle distribution. Significant increases in rates of cells in the G1 phase were seen but remarkable reductions in those of cells in the S phase were found in the MCPH1 mimic subset versus the Blank and NC subsets (all P<0.05). Rate of cells in the G1 phase dropped strikingly but that of cells at the S phrase rose remarkably in the siRNA-MCPH1 subset (P<0.05).

Chemo-sensitivity

IC_{50} values of cells in the remaining subsets were substantially higher than that of cells in the Normal group (all P<0.05). Compared to Blank and NC subsets, IC_{50} values of cells were lowered remarkably in the MCPH1 mimic subset (both P<0.05) but elevated strikingly in the siRNA-MCPH1 subset (both P<0.05) (**Table 5**). IC_{50} values of cells in the remaining subsets rose considerably versus that of cells in the Normal subset, indicating that sensitivity of cells to chemotherapy was reduced remarkably in the remaining subsets. After cells of non-small cell lung cancers had been transfected with MCPH1 overexpression plasmids, IC_{50} was decreased. This implied that the cells were sensitive to chemotherapy and that, to some extent, MCPH1 can increase sensitivity of cells to chemotherapy.

Discussion

MCPH1 genes are essential genes for monitoring the mitosis of human cells [11]. MCPH1 has been shown to be closely linked with repairing DNA damage. It can regulate DNA damage response pathways, be involved in repair of cell damage, and monitor cell cycling to ensure genomic stability [12-15]. One study exploring the association between breast cancer and MCPH1 genes demonstrated that, after knockout of MCPH1 gene in mice, genomic instability increased and mice were more likely to develop breast tumors [16]. This further suggests that low expression or absence of MCPH1 plays a crucial role in presenting and progression of tumors. Additionally, expression of MCPH1 genes is downregulated in lung cancer tissues compared with that of normal tissue, indicating that, as a tumor suppressor, MCPH1 is para-

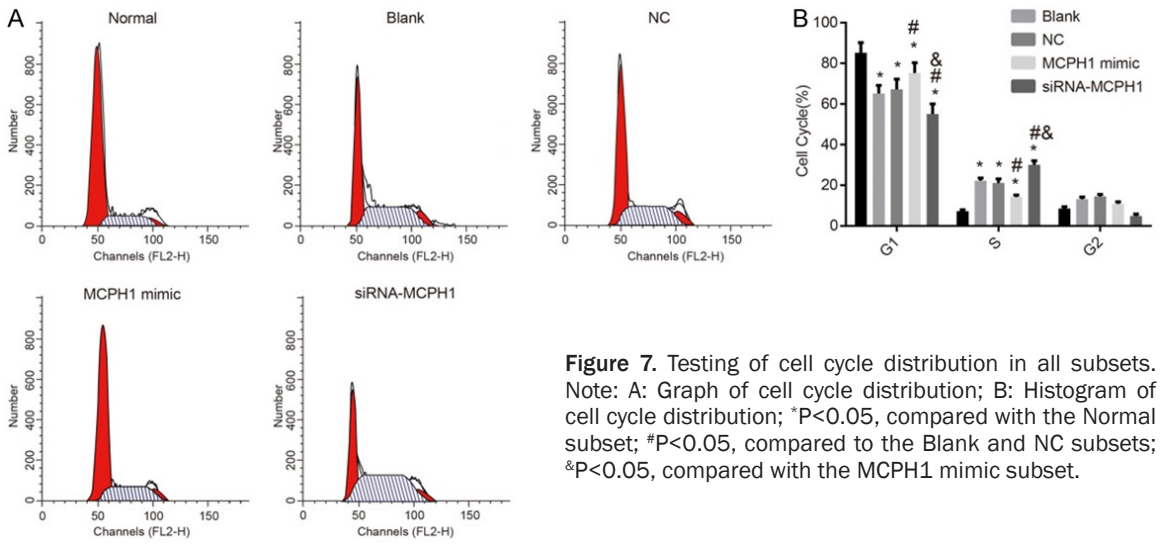

Figure 7. Testing of cell cycle distribution in all subsets. Note: A: Graph of cell cycle distribution; B: Histogram of cell cycle distribution; *P<0.05, compared with the Normal subset; #P<0.05, compared to the Blank and NC subsets; &P<0.05, compared with the MCPH1 mimic subset.

mount in the development of lung cancer [17, 18].

Immunohistochemical staining revealed that positive rates of MCPH1 in cancer tissues were considerably lower than that in normal tissues, consistent with the findings of Golubeva et al. This suggests that MCPH1 is lowly expressed in cancer tissues [19]. CGH analysis of changes in genomic DNA sequences in 50 specimens of non-small cell lung cancers demonstrated that almost every case among the specimens was implicated in chromosomal aberrations. Karami and Kopparapu et al. found that, as a DNA repair gene, downregulation of MCPH1 in cancer tissue is associated with higher risk for genomic instability and poses problems to cell division [20, 21]. This might also be a decisive cause for abnormal genomic DNA sequences in specimens of non-small cell lung cancers and remarkably higher LOH of MCPH1 in cancer tissue than normal tissue. qRT-PCR and Western blot assays revealed that, when compared to Blank and NC subsets, mRNA expression levels of MCPH1 and Bax rose but those of PARP1, PRKDC, POLD1 and Bcl-2 dropped substantially in the MCPH1 mimic subset; mRNA expression levels of MCPH1 and Bax decreased remarkably but those of PARP1, PRKDC, POLD1, and Bcl-2 were elevated significantly in the siRNA-MCPH1 subset, implying that silencing of MCPH1 expression can considerably elevate expression of proliferation-associated genes (PARP1, PRKDC, POLD1 and Bcl-2) and inhibit expression of apoptosis-associated gene Bax in cells of non-small cell lung cancers. Moreover, MTT and Annexin V-FITC/PI double staining assays further validated the role of low-expression of MCPH1 in promoting proliferation of cells of non-small cell lung cancers and accelerating diffusion of cancer cells. Liang reported that MCPH1 genes have low-expression in a sea of tumor tissues, including those of breast cancer and ovarian cancer. Furthermore, proliferation of tumor tissues further accelerated, division was significantly reduced, and the balance of cell proliferation and apoptosis was further lost [22]. This was confirmed as this study determined expression of MCPH1 in lung cancer tissues.

After addition of cisplatin and paclitaxel to all cell subsets, compared with Blank and NC subsets, IC_{50} value of cells was decreased remarkably in the MCPH1 mimic subset but rose considerably in the siRNA-MCPH1 subset. These results suggest that, after transfection of MCPH1 over-expression plasmids in cells in non-small cell lung cancers, the cells are more sensitive to chemotherapy and MCPH1, to a certain degree, can increase the sensitivity of cells to chemotherapy.

In conclusion, silencing of MCPH1 genes can promote proliferation of cells of non-small cell lung cancers, inhibit their apoptosis, and reduce their sensitivity to cisplatin chemotherapy. This study lays a theoretical basis for a better understanding of the molecular mechanisms of MCPH1 associated with lung cancer and brings some insight into the targeted man-

agement of non-small cell lung cancers. The findings, however, need further validation by relevant *in vivo* experiments and toxicity trials. Overall, this study confirms association between silencing of MCPH1 genes and cell proliferation and apoptosis in non-small cell lung cancers, but only from the perspective of genes. The specific underlying mechanisms, however, still require further exploration.

Acknowledgements

This work was supported by the Natural Science Foundation of Shandong Province (ZR-2015HL072).

Disclosure of conflict of interest

None.

Address correspondence to: Li Wei, Department of Respiratory Medicine, Affiliated Hospital of Taishan Medical University, No. 706 Taishan Street, Taian City 271000, Shandong Province, P. R. China. Tel: +86-0538-6233055; E-mail: weili2589@163.com

References

[1] Bhattacharya N, Mukherjee N, Singh RK, Sinha S, Alam N, Roy A, Roychoudhury S and Panda CK. Frequent alterations of MCPH1 and ATM are associated with primary breast carcinoma: clinical and prognostic implications. Ann Surg Oncol 2013; 20 Suppl 3: S424-432.

[2] Zhang J, Wu XB, Fan JJ, Mai L, Cai W, Li D, Yuan CF, Bu YQ and Song FZ. MCPH1 protein expression in normal and neoplastic lung tissues. Asian Pac J Cancer Prev 2013; 14: 7295-7300.

[3] Garciacampelo MR, Taron M, Benlloch S, Sanchez JJ, Costa C, Capitan AG, Bertranalamillo J, Mayo C, Molinavila MA and Majem M. MCPH1 (BRIT1) and outcome to erlotinib in non-small cell lung cancer (NSCLC) patients (p) harboring EGFR mutations. Annals of Oncology 2012; 23: 533.

[4] Zhou L, Bai Y, Li Y, Liu X, Tan T, Meng S, He W, Wu X and Dong Z. Overexpression of MCPH1 inhibits uncontrolled cell growth by promoting cell apoptosis and arresting the cell cycle in S and G2/M phase in lung cancer cells. Oncol Lett 2016; 11: 365-372.

[5] Venkatesh T and Suresh PS. Emerging roles of MCPH1: expedition from primary microcephaly to cancer. Eur J Cell Biol 2014; 93: 98-105.

[6] Hemmat M, Rumple MJ, Mahon LW, Morrow M, Zach T, Anguiano A, Elnaggar MM, Wang BT and Boyar FZ. CMA analysis identifies homozygous deletion of MCPH1 in 2 brothers with primary microcephaly-1. Mol Cytogenet 2017; 10: 33.

[7] Pulvers JN, Journiac N, Arai Y and Nardelli J. MCPH1: a window into brain development and evolution. Front Cell Neurosci 2015; 9: 92.

[8] Mantere T, Winqvist R, Kauppila S, Grip M, Jukkola-Vuorinen A, Tervasmaki A, Rapakko K and Pylkas K. Targeted next-generation sequencing identifies a recurrent mutation in MCPH1 associating with hereditary breast cancer susceptibility. PLoS Genet 2016; 12: e1005816.

[9] Wenting HE. Detection of MCPH1 mRNA expression in lung cancer and the effect of MCPH1 overexpression synergistic with chemotherapeutic drugs on tumor inhibition rate of A549 cells. Basic & Clinical Medicine 2014.

[10] Yong HJ, Choi YE, Park HM and Yoon K. Abstract 1221: apoptosis is regulated by MCPH1 via p38 MAPK. Cancer Research 2010; 70: 1221.

[11] Aberle DR, Adams AM, Berg CD, Black WC, Clapp JD, Fagerstrom RM, Gareen IF, Gatsonis C, Marcus PM and Sicks JD. Reduced lung-cancer mortality with low-dose computed tomographic screening. N Engl J Med 2011; 365: 395-409.

[12] Kwak EL, Bang YJ, Camidge DR, Shaw AT, Solomon B, Maki RG, Ou SH, Dezube BJ, Janne PA, Costa DB, Varella-Garcia M, Kim WH, Lynch TJ, Fidias P, Stubbs H, Engelman JA, Sequist LV, Tan W, Gandhi L, Mino-Kenudson M, Wei GC, Shreeve SM, Ratain MJ, Settleman J, Christensen JG, Haber DA, Wilner K, Salgia R, Shapiro GI, Clark JW and Iafrate AJ. Anaplastic lymphoma kinase inhibition in non-small-cell lung cancer. N Engl J Med 2010; 363: 1693-1703.

[13] Liu X, Zong W, Li T, Wang Y, Xu X, Zhou ZW and Wang ZQ. The E3 ubiquitin ligase APC/CCdh1 degrades MCPH1 after MCPH1-Î²TrCP2-Cdc-25A-mediated mitotic entry to ensure neurogenesis. EMBO J 2017; 36: 3666-3681.

[14] Kleiner RE, Verma P, Molloy KR, Chait BT and Kapoor TM. Chemical proteomics reveals a gamma H2AX-53BP1 interaction in the DNA damage response. Nat Chem Biol 2015; 11: 807-814.

[15] Awaji AA, Shaaban A, Shukla S, Bond J, Morrison E, Cookson V and Bell S. 55PE valuation of the role of MCPH1 and p53 expression in response to chemotherapy and subsequent survival in breast cancer. Annals of Oncology 2015; 26: iii19.

[16] Liu X, Zhou ZW and Wang ZQ. The DNA damage response molecule MCPH1 in brain development and beyond. Acta Biochim Biophys Sin (Shanghai) 2016; 48: 678-685.

[17] Ghafouri-Fard S, Fardaei M, Gholami M and Miryounesi M. A case report: autosomal recessive microcephaly caused by a novel mutation in MCPH1 gene. Gene 2015; 571: 149-150.
[18] Mai L, Yi F, Gou X, Zhang J, Wang C, Liu G, Bu Y, Yuan C, Deng L and Song F. The overexpression of MCPH1 inhibits cell growth through regulating cell cycle-related proteins and activating cytochrome c-caspase 3 signaling in cervical cancer. Mol Cell Biochem 2014; 392: 95-107.
[19] Golubeva VA, Woods NT and Monteiro ANA. Abstract 3779: mutational analysis of MCPH1 C-terminal tandem BRCT domain reveals residues essential for cell cycle arrest. Cancer Research 2015; 75: 3779.
[20] Karami F, Javan F, Mehrazin M and Mehdipour P. Key role of promoter methylation and inactivation of MCPH1 gene in brain tumors. Journal of Neurology Research 2015; 4: 132-137.
[21] Kopparapu PK, Miranda C, Fogelstrand L, Mishra K, Andersson PO, Kanduri C and Kanduri M. MCPH1 maintains long-term epigenetic silencing of ANGPT2 in chronic lymphocytic leukemia. FEBS J 2015; 282: 1939-1952.
[22] Liang Y, Gao H, Lin SY, Goss JA, Du C and Li K. Mcph1/sol Brit1 deficiency promotes genomic instability and tumor formation in a mouse model. Oncogene 2015; 34: 4368-4378.